Journal of Orthopaedic Translation (2016) 5, 38—47

Available online at www.sciencedirect.com

ScienceDirect

journal homepage: http://ees.elsevier.com/jot

ORIGINAL ARTICLE

Assessment of activated porous granules on implant fixation and early bone formation in sheep

Ming Ding [a,*,1], Susan S. Henriksen [a,1], Naseem Theilgaard [b], Søren Overgaard [a]

[a] *Orthopaedic Research Laboratory, Department of Orthopaedic Surgery and Traumatology, Odense University Hospital, Institute of Clinical Research, University of Southern Denmark, Odense C, Denmark*
[b] *Danish Technological Institute, Plastics Technology, Taastrup, Denmark*

Received 29 June 2015; received in revised form 2 August 2015; accepted 22 September 2015
Available online 29 October 2015

KEYWORDS
BMSC;
histomorphometry;
implant fixation;
microarchitecture;
porous scaffold granules;
3-dimensional perfusion bioreactor

Summary *Background/Objective:* Despite recent progress in regeneration medicine, the repair of large bone defects due to trauma, inflammation and tumor surgery remains a major clinical challenge. This study was designed to produce large amounts of viable bone graft materials in a novel perfusion bioreactor to promote bone formation.
Methods: Cylindrical defects were created bilaterally in the distal femurs of sheep, and titanium implants were inserted. The concentric gap around the implants was randomly filled either with allograft, granules, granules with bone marrow aspirate (BMA) or bioreactor activated granule (BAG). The viable BAG consisted of autologous bone marrow stromal cells (BMSCs) seeded upon porous scaffold granules incubated in a 3D perfusion bioreactor for 2 weeks prior to surgery. 6 weeks after, the bone formation and early implant fixation were assessed by means of micro-CT, histomorphometry, and mechanical test.
Results: Microarchitectural analysis revealed that bone volume fraction and trabecular thickness in the allograft were not statistically different than those (combination of new bone and residue of granule) in the other 3 groups. The structure of the allograft group was typically plate-like, while the other 3 groups were combination of plate and rod. Histomorphometry showed that allograft induced significantly more bone and less fibrous tissue in the concentric gap than the other 3 granule groups, while the bone ingrowth to implant porous surface was

* Corresponding author. Orthopaedic Research Laboratory, Department of Orthopaedic Surgery and Traumatology, Odense University Hospital, Winsløwparken 15, 3.sal, DK-5000, Odense C, Denmark.
E-mail address: ming.ding@rsyd.dk (M. Ding).
[1] These authors contributed equally to this paper, and should both be considered as first authors.

http://dx.doi.org/10.1016/j.jot.2015.09.008

not different. No significant differences among the groups were found regarding early implant mechanical fixation.
Conclusion: In conclusion, despite nice bone formation and implant fixation in all groups, bioreactor activated graft material did not convincingly induce early implant fixation similar to allograft, and neither bioreactor nor by adding BMA credited additional benefit for bone formation in this model.

Introduction

The early bone ingrowth to porous surface of implants increases primary implant fixation and reduces the risk of implant failure [1]. Osseointegration is influenced by the primary mechanical stability and secondary biological stability after bone remodelling of the implant in the bone. Thereby, early bone formation and apposition is essential for secondary stability [2].

Despite recent progress in regeneration medicine, the repair of large bone defects due to trauma, inflammation, and tumour surgery remains a major clinical challenge. Large animal models have been developed to test bone repair by tissue engineering approaches that combines the principles of engineering and life sciences to overcome drawbacks of traditional bone regeneration techniques used in orthopaedics [3]. These new techniques are intended to develop the tissue-engineered constructs with similar structural and mechanical characteristics of natural bone [4]. In general, an advantage in the bone regeneration in large defect has often been reported when scaffolds were seeded with bone marrow derived stromal cells (BMSCs) [5].

Consequently, bioreactor is introduced. This device enables a closely monitored and tightly controlled environment to allow biological and biochemical processes. Bone tissue engineering consists of static cultures, in which bone cells are seeded on a 3-dimensional (3D) scaffold and placed in a well-plate for a certain period of time. This culture strategy leads to significant drawbacks that the cells tended to accumulate at the periphery of the scaffold leading to poor nutrient and waste exchange in the centre of the scaffold [6]. Furthermore, cell necrosis could also be formed in the centre of the scaffold. Dynamic bioreactors such as perfusion bioreactors might overcome such problems in cell culture.

A perfusion bioreactor is developed and designed to mimic the microscopic mechanical loading of bone *in vivo* [7]. Perfusion bioreactor systems automatically pump culture medium through the interconnected pores of scaffold that is press-fitted into a culture chamber [8—10]. With flow perfusion, the mass transfer is enhanced at the interior of the 3D scaffold and shear forces are applied to the cultured cells. Compared with other bioreactor systems, a perfusion bioreactor increases mass transport leading to improved distribution of extracellular matrix throughout the 3D scaffold, increased cell number, enhanced expression of the osteogenic phenotype, and improved mineralized extracellular matrix deposition [9,11,12]. It is worth noting that only the perfusion bioreactor is able to eliminate diffusion limitations inside a scaffold, although dynamic bioreactors can overcome diffusion limitations at the surface of a scaffold [9,13]. Hence, the perfusion bioreactor seems to be a very useful dynamic culture technique for bone tissue engineering [4,6], and is the current most commonly used dynamic bioreactor [14].

This study was designed to produce viable bone graft material for early fixation of titanium alloy implants to bone defects. The procedures described and used aimed at mimicking the possible future clinical setting, where autologous BMSCs were harvested and implanted with a biomaterial around a critical defect created in association with a revision of a total joint arthroplasty (fluidised bed concept). We hypothesised that filling with the bioreactor activated graft material (BAG) in a 2 mm defect in sheep bone would result in ingrowth and bone formation comparable to allograft.

Materials and methods

Study design

This study used a well-validated bilateral implant-gap defect model that has been described in detail previously [15,16]. Eight sheep were included based on sample size calculation and our previous experience. Cylindrical defects were created laterally and medially in the bilateral distal femoral condyles of each sheep. This allowed bilateral insertion (press fit) of titanium alloy implants extra-articularly in the distal femurs; thus, four implants per sheep. The concentric defect around the inserted titanium alloy implant was filled with one of the four materials: (1) allograft serving as control; (2) granule; (3) granules incubated with fresh autologous bone marrow aspirate (BMA); or (4) granules incubated for 2 weeks in a bioreactor with autologous BMSCs. The filling materials were alternated between insertion holes in order to avoid any site dependent differences. This randomisation allowed all four materials to be implanted medially or laterally within the same sheep.

Animals and bone marrow aspiration

This study was approved by the Danish Animal Experiments and Inspectorates (no. 2008/561-1544), and all animal

experiments were performed in accordance with the animal research guidelines. Eight skeletally mature female ewes (mean age 4 y) of Merino/Gotland mixed breed were used. The sheep were not bred for experimental purposes, but bought for the experiment from a local farmer. Mean weight was 77.9 ± 11.0 kg. The animals were housed in facilities provided by the Biomedical Laboratory at the University of Southern Denmark, Odense, Denmark. A limited amount of compound feed was provided together with free access to water, straw, and hay. All efforts were made to minimise animal suffering.

Bone marrow (4 × 5 mL) was aspirated from the iliac crest of the eight anaesthetised sheep. Xylazine (0.01 mL/kg Rompun Vet, Bayer, Leverkusen, Germany) was given, followed by propofol (1 mg/kg; Rapinovet, Schering-Plough, Ballerup, Denmark). Two millilitres of lidocaine (Amgros, Copenhagen, Denmark) was applied to the posterior iliac crests prior to aspiration for local anaesthesia. The aspirates were immediately transferred to Falcon tubes containing Gibco's α-minimal essential medium (Gibco's α-MEM+, Invitrogen, Taastrup, Denmark) with 1 mL 5000 I.U./mL heparine (Nycomed, Copenhagen, Denmark). On indication, 2 mL of 0.03 mg/mL buprenorphine (Temgesic, Schering-Plough, Ballerup, Denmark) was given intramuscularly.

Isolation of mononuclear cells

Mononuclear cells were isolated using density gradient centrifugation through a Histopaque gradient (Sigma-Aldrich, Brøndby, Denmark). The total amounts of isolated cells from each sheep were resuspended in 22 mL of fresh α-MEM+ before injection into a perfusion bioreactor (Millenium Biologix AG, Zurich, Switzerland).

Fibroblastic colony forming units assay

The osteogenic potential of the mononuclear cells were evaluated by a fibroblastic colony forming unit (CFU-f) assay according to previous studies [8,17]. The fractions of clonogenic fibroblastic cells in the total amount of isolated mononuclear cells were determined using a CFU-f assay. From the isolated cells, 10^5 cells were aspirated and resuspended in 15 mL α-MEM+ before plating in T-80 flasks. Then, the flasks were incubated until the cells reached confluence or colonies were visible (at 2 weeks). Incubation media was changed weekly, thereby washing off any unattached cells, and thus keeping only living cells of the mesenchymal lineage. Following incubation, the media was aspirated and the cells were fixed in 4% buffered formalin before staining with crystal violet for approximately 30 minutes. Crystal violet was aspirated and the CFU-f was counted [8].

Perfusion bioreactor

The perfusion bioreactor was developed by Millenium Biologix AG (Basel, Switzerland) as part of the European project "AUTOBONE", the Sixth European Framework Program (Project "AUTOBONE", Grant No. NMP3-CT-2003-505711). The 3D perfusion bioreactor system is described in detail in a recent publication [18]. The cylindrical scaffold chambers (diameter = 0.9 cm) were modified for this study; thus containing 1 mL of scaffold granules.

Scaffold granules within the chamber were perfused twice with 22 mL α-MEM+ 2 hours prior to injection of isolated cells ("washing" step). The cell was resuspended in 22 mL of fresh α-MEM+ before injection into the perfusion bioreactor. The bioreactor ran a "seeding" step for 4 days with a perfusion flow of 40 mL/min. Hereafter, fresh α-MEM+ supplemented with 10nM dexamethasone, 0.1mM L-ascorbic-acid-2-phosphate, and 5 ng/mL fibroblast growth factor-2 were injected into the perfusion bioreactor every 3rd or 4th day, starting 4 days after bioreactor incubation was initiated [18,19]. After the initiation phase, the perfusion flow was reduced to 4 mL/min for the remaining incubation time. Throughout the 2 weeks incubation period, the perfusion bioreactor was placed inside an incubator (37°C, 5% CO_2) [18].

Titanium alloy implants

A total of 32 plasma-sprayed, porous titanium alloy implants were used (90% titanium, 6% aluminium, 4% vanadium; kindly donated by Biomet, Warsaw, IN, USA). The implants were cylindrical with a height of 10 mm and an inner column diameter of 6 mm. Attached with a footplate and top washer, both 10 mm in diameter; thus resulting in a circumferential gap of 0.5 mL. The porous surface had a mean porosity of 44% and a mean pore diameter of 480 μm (as specified by the manufacturer) [8].

Graft materials

Allograft

Morselized allograft (Ø 200–600 μm) was prepared from bone harvesting from the distal femurs and proximal tibias of a skeletally mature healthy female sheep at least 6 months prior to surgery. Sterile vials containing 1 mL allograft were kept at −80°C until the day of surgery.

Scaffold granules

Scaffold granules (Ø 1000–1500 μm, 88 % porosity), consisting of hydroxyapatite (HA) 70% and β-tricalcium-phosphate (β-TCP) 30%, were supplied by the Danish Technological Institute. The organic polymer (PDLLA)-reinforced HA/β-TCP contained 88% inorganic ceramic (70% HA and 30% β-TCP) and 12% PDLLA by weight. An ultra-thin layer of PDLLA was infiltrated on the surface of the pores, and kept intermicropore connections [20]. These granules were coated with a polymer in order to increase the mechanical strength of the newly formed bone [21]. The polymer was [50% polylactic acid (D-PLA), 50% L-PLA] poly-lactic acid (PDLLA) 12.5%, and its molecular weight was 308 kDa (Phusis, Saint Ismier, France). The pore sizes were 300–700 μm, and interconnecting pore sizes were 100–200 μm.

Scaffold granules with BMA

During surgery, 2 mL of freshly aspirated autologous BMA was aspirated from the proximal tibia. The BMA was quickly mixed with the scaffold granules in a sterile petri dish before filling around the titanium alloy implant.

Bioreactor activated granule material (BAG)
The BAG was incubated for 2 weeks in the perfusion bioreactor with autologous mononuclear cells as described above. On the day of surgery, the bioreactor had finished the 2 weeks incubation period, and the BAG material was filled around the critical sized defect created in the distal femur as described below.

Surgical procedure and implantation model

Surgical procedures were performed under general anaesthesia. The sheep were premedicated with xylazine (10 mL/kg; Rompun Vet; Bayer) and intravenous injection of propofol (1 mg/kg; Rapinovet; Schering-Plough) on indication. A bolus injection of 2 mL 0.03 mg/mL buprenorphine (Temgesic; Schering-Plough) was given as prophylactic analgesia. The sheep were intubated in order to maintain general anaesthesia by inhalation of 2.0% isoflurane during surgery (Siesta Vet, Dameca, Denmark).

An implant-gap defect model was applied to the bilateral distal femurs of all sheep. After shaving and disinfection of the skin, the distal femur condyle was exposed by a lateral incision. A guide K-wire was used perpendicularly to the surface of the condyle, a central guide hole was drilled before drilling a 12 mm deep cylindrical hole first with a sharp drill then with a flat drill. The drill hole was rinsed with 20 mL saline, and titanium alloy implants were press-fit inserted into the cylindrical defects. The concentric gap (0.5 mL) surrounding the titanium implant was filled with allograft, scaffold granules, scaffold granules with fresh BMA, or BAG material according to a randomised scheme. The gap was closed with a top washer. The ligaments were tightly sutured over the defect, and the wounds were closed with sutures in three layers. The same procedure was repeated for the medial side and for the opposite femur [22].

Three times daily 2.0 mL 0.03 mL/mg buprenorphine (Temgesic; Schering-Plough), and once daily 9.0 mL 250 mg/mL ampicillin (Ampivet Vet, Boehringer Ingelheim, Denmark) were given for 6–7 days postoperatively. The sheep were allowed to move freely around, and most of the sheep were already walking/standing 2 hours after surgery. Six weeks after surgery, the sheep were euthanized with an overdose of pentobarbital.

Preparation of bone specimens

The distal femurs were harvested and stored at −20°C until further processing. Soft tissues were carefully cleared off the specimens, and the femur condyles were sawed in two parts—lateral and medial on a continuing water irrigation Exact diamond band saw (Apparatebau, GmbH, Germany). The top washer was sawed off; hereafter, a second saw was made to create a bone-implant specimen with a thickness of 3.5 mm. These bone-implant specimens were immediately frozen and stored at −20°C, before undergoing microcomputed tomography (μCT) scanning and further mechanical testing. The remaining part of the bone-implant specimen was sawed to a thickness of 6 mm for histomorphometry [8].

The latter 6 mm specimens were transferred to graded ethanol (70–100%) containing basic fuchsin for dehydration. Following dehydration, the specimens were fixed in methylmetacrylate (Technovit 9100 NEW; Heraus Kulzer GmbH, Germany). The vertical sectioning method was applied to prepare 30 μm thick sections for histomorphometric analyses [23]. The sections were sawed on a custom-made microtome (Instrumentmakerij, Medeja, The Netherlands), and were counterstained with 2% light green for 2 minutes, rinsed, and mounted on glass slides. Four sections were sawed out of each bone-implant specimen; resulting in 16 sections per sheep and ultimately 128 sections overall [8].

Microtomographic scanning

The bone-implant specimens were scanned using a high resolution μCT system (viva CT-40; Scanco Medical AG, Brüttisellen, Switzerland) using 70 kV energy and 85 μA intensity [24]. All specimens were scanned using the same scanning protocol settings and in the same orientation. After μCT scanning, a volume of interest for each bone specimen was defined as the concentric gap surrounding the implant, i.e., starting from the surface of the titanium alloy implant and ending at 2000 μm to the host bone. The scanned images resulted in 3D reconstruction cubic voxel sizes of $10.5 \times 10.5 \times 10.5\ \mu m^3$ ($2048 \times 2048 \times 2048$ pixels). An optimal global threshold of 200 was applied to segment μCT images using the segmentation techniques described in detail previously [25], with a slight modification to obtain accurate 3D imaging datasets [26].

The following parameters were chosen for assessing microarchitecture of the graft materials and bone within the volume of interests after implantation: bone-$\pm$substitute volume density [25], trabecular thickness (TbTh) [27], structure model index (SMI) [28], and connectivity density (CD) [29].

These microarchitectural parameters were chosen as quantitative assessments of the bone regeneration within the concentric gap. Bone $\pm$ substitute volume density describes the formation of bone. SMI characterises the 3D structure types of the scaffold consisting of certain amount of rods and plates. The value of SMI lies between 0 and 3, when the structure consists of both rods and plates of equal thickness, depending on the volume ratio of rods and plates. An ideal plate-like structure will reflect a high mechanical strength and has a SMI value of 0, whereas an ideal rod-like structure will reflect a low mechanical strength and has a SMI value of 3 [28,30]. CD is a topological measurement used to describe the number of multiple interconnected scaffold trabeculae within the material [29]. TbTh is also an important characteristic and directly related to the mechanical strength of the bone-scaffold construct.

Histomorphometry

Stereological software (newCAST; Visiopharm, Denmark) applying linear interception technique was used to quantify tissue ingrowth at the titanium implant-material surface [31]. The area fractions of bone, fibrous tissue, miscellaneous, marrow, and substitute granules of the blinded sections were quantified with the linear interception technique. The area fraction of bone was quantified as "all bone" (including allograft and new bone).

Tissue volume in two predefined regions of interest in the gap between the titanium implant and host bone was quantified: Zone 1: from the titanium implant surface and 500 μm away into the grafted defect; and Zone 2: from 500–2000 μm into the grafted defect. The zones are described in a current study by Babiker et al [32]. The volume fractions of bone, fibrous tissue, miscellaneous, marrow, and substitute granules of the blinded sections were quantified by point-counting technique [33]. The sampling probe and size were defined in order to sample 100 "hits" for bone per implant site as previously described [23].

Mechanical testing

The bone specimens were thawed at room temperature 2 hours prior to mechanical testing. All specimens were blinded and tested the same day under the same conditions on an 858 Bionix MTS hydraulic material testing system (MTS Systems Co., Minneapolis, MN, USA) using a 1kN load cell. A preload of 2N defined the contact position for the test. The implants were pushed out of the surrounding bone in the direction of the implant axis. The displacement rate was 5 mm/minute. Load versus displacement data were recorded and converted to stress and strain data to calculate shear mechanical properties between implant and host bone—shear stiffness (MPa), maximum shear strength (MPa), and failure energy (kJ/cm^2).

Statistical analysis

Results from μCT scanning were analysed with one-way analysis of variance, following a *post hoc* Tukey's test when appropriate. Differences between group means were considered statistically significant when p values were less than 5%.

Data sets from mechanical testing and histomorphometry were not normally distributed; therefore, differences between group medians were tested using Kruskal–Wallis nonparametric analysis of variance by ranks. All data from mechanical testing were presented with the median indicated. For histomorphometric data, median and interquartile ranges were given. Outliers were excluded based on the Interquartile Method, where the value s is an outlier if $s < 1$. Quartile - 1.5 × interquartile range or $s > 3$. Quartile + 1.5 × interquartile range. Differences between group medians were considered statistically significant when p values were less than 5%.

The sample size calculation was based on previous studies using histomorphometric and mechanical data for the assessment of early implant fixation in large animal models [34–36]. The number of sheep included in this study was based on a sample size calculation, for a paired study design:

$$n = (t_{2\alpha} + t_{\beta})^2 * \frac{SD^2}{D^2} \quad (1)$$

where α is the risk of a type I error and β is the risk of a type II error. The critical value for 2α is 1.96 for a confidence level of 95%. The critical value for β is 0.84, due to the selected power (1-β) = 80%. The minimal clinically relevant difference, D is set to 70%. The standard deviation was set to 50% for mechanical and histological data. Based on the calculation above, at least six sheep per study should be included in each study; thus, eight animals were included for each scaffold material.

Results

No postoperative complications were seen, and all sheep were able to stand or walk around approximately 2 hours after surgery. No clinical signs of infections were observed during the observation period of 6 weeks. One implant (sheep 6) was loosened from the drilled defect during the observation period; thus it was excluded from further analyses. Outliers were also excluded from the push-out data. Of the eight sheep, only five met the minimum number of CFU-f for bone, and three CFU-f levels were too low [37]. The total amounts of CFU-fs are reported in Table 1.

3D microarchitecture

Microarchitectural analysis of bone formation in the concentric gap revealed relatively less bone formation in the granule + BMA group than in the other groups, but this was not statistically significant (Table 2). No significant differences in the TbTh and CD were observed among the four groups. The allograft had a more plate-like structure, the granules, and BAG groups had a combination of plate and rod structure, while the structure in the granule + BMA group was more rod-like (Table 2, Figure 1).

Histomorphometry

Tissue volume

Quantification of tissue volumes revealed a significantly ($p < 0.05$) greater bone formation in the allograft group in both Zones 1 and 2 than the other three groups, while there were no significant differences among the other three groups (Table 3). Furthermore, in Zone 2, the allograft group had significant less fibrous tissue formation compared with the other three groups ($p < 0.05$). The residual of scaffold granules were not significantly different among the three groups (Table 3).

Table 1 Total number of fibroblastic colony forming units obtained from the bone marrow aspirate of each sheep.

Sheep no.	Total no. of initial CFU-f	Meets the estimated minimum no. of CFU-f for bone (5.200–7.500) Braccini et al [17]
1	2241	No
2	33,024	OK
3	28,672	OK
4	6552	Minimum
5	322	No
6	35,872	OK
7	22,848	OK
8	992	No

CFU-f = fibroblastic colony forming units.

Table 2 Microarchitectural parameters of bone (substitute) mass in concentric gap between implant and host bone for the four groups.

	BV/TV (%)[a]	TbTh (μm)[a]	SMI (−)[a]	CD (−)[a]
Allograft ($n = 8$)	44.3 ± 10.0	67.6 ± 7.9	0.3 ± 1.5	867.1 ± 148.7
Granules ($n = 8$)	39.7 ± 5.7	67.2 ± 5.4	1.8 ± 0.7	930.1 ± 120.2
Granules + BMA ($n = 7$)	34.9 ± 4.0	65.1 ± 3.8	2.3 ± 0.4	825.1 ± 109.7
BAG ($n = 8$)	45.0 ± 11.8	98.8 ± 84.1	1.2 ± 1.3	930.2 ± 188.2
p* (ANOVA)	$p = 0.11$	$p = 0.37$	$p < 0.009$ Allograft < Granule + BMA	$p = 0.44$

ANOVA = analysis of variance; BAG = bioreactor activated graft material; BMA = bone marrow aspirate; BV/TV = bone ± substitute volume density; CD = connectivity density; SMI = structure model index; TbTh = trabecular thickness.
* Differences between means were considered statistically significant for p values less than 0.05.
[a] Data are presented as mean ± standard deviation.

Ingrowth

Histomorphometry revealed no significant differences between allograft and the other materials regarding ingrowth (Table 4). The BAG seemed to induce less fibrous tissue at the implant—tissue interface as compared to the other materials; however, this difference was not statistically significant (Table 4).

Histology

Histological observations of the tissue—implant interface supported the results from the histomorphometric analyses and push-out tests (Figure 2). Unresorbed scaffold granules were seen in all slides, except for the allograft group. Fibrous tissue encapsulation of the implant with minimal bone formation was also seen.

Large amounts of bones, lamellar, and woven, were observed in the allograft group, and the amounts of bone seen in these specimens were largely concentrated in Zone 2. Similar observations were noticed for all other graft material-bone tissue, and were largely seen in Zone 2. Nonresorbed scaffold granules could be seen in all specimens implanted with either granule alone, with BMA or as BAG material. Ossicles were observed in specimens treated with BAG material.

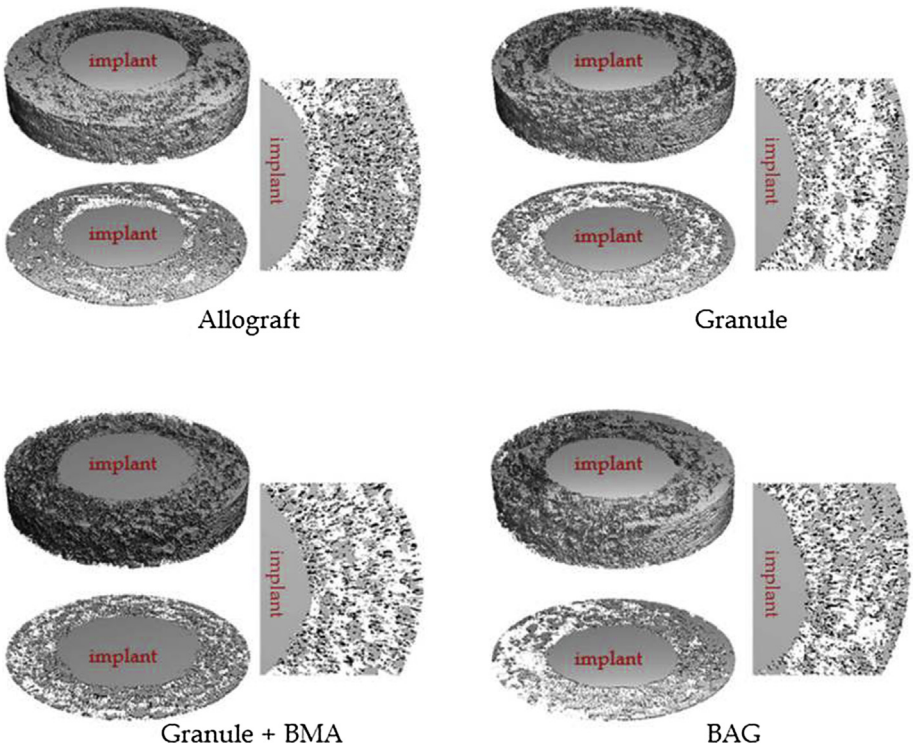

Figure 1 Three-dimensional reconstruction of micro-computed tomography images of four groups in the same sheep. Significant bone formation could be seen in the concentric gaps around the porous surface of the titanium implant in all groups, and the newly formed bone ingrowth to the porous surface of implant could also be observed, which determined mechanical fixation strength. BAG = bioreactor activated graft material; BMA = bone marrow aspirate.

Table 3 Histomorphometric analyses of tissue volumes, bone, fibrous tissue, and scaffold granules.

	Tissue volume/total tissue (%)	Bone[a]	Fibrous tissue[a]	Scaffold granules[a]
Zone 1	Allograft ($n = 6$)	28.3 (23.3–35.5)	21.0 (13.0–39.5)	—
	Granules ($n = 7$)	13.0 (8.9–25.2)	52.3 (43.0–54.2)	19.9 (17.6–22.4)
	Granules + BMA ($n = 6$)	7.2 (6.3–18.1)	42.0 (35.3–56.5)	24.4 (16.6–29.0)
	BAG ($n = 7$)	9.7 (7.5–13.1)	38.4 (37.2–51.1)	23.4 (21.1–26.7)
	p*	$p < 0.05$	$p = 0.186$	$p = 0.390$
	(Kruskal–Wallis)	Allograft > all		
Zone 2	Allograft ($n = 6$)	42.0 (35.2–44.5)	8.5 (2.7–12.7)	—
	Granules ($n = 7$)	24.4 (22.3–26.9)	25.1 (18.3–35.0)	19.6 (13.0–24.0)
	Granules + BMA ($n = 6$)	14.0 (5.5–23.7)	33.6 (23.3–39.4)	27.3 (18.6–32.4)
	BAG ($n = 7$)	12.1 (7.7–20.4)	37.7 (35.2–42.5)	24.6 (20.3–34.1)
	p*	$p < 0.05$	$p < 0.05$	$p = 0.362$
	(Kruskal–Wallis)	Allograft > all	Allograft < all	

BAG = bioreactor activated graft material; BMA = bone marrow aspirate.
* Differences between medians were considered statistically significant for p values less than 0.05.
[a] Data are presented as median (range).

Table 4 Histomorphometric analyses of tissue ingrowth to the porous surface of implant presented as a percentage of total surface area: bone, fibrous tissue, and substitute.

Tissue ingrowth/total tissue (%)	Bone[a]	Fibrous tissue[a]	Scaffold granules[a]
Allograft ($n = 7$)	18.8 (17.6–24.7)	75.0 (64.3–78.6)	—
Granules ($n = 6$)	20.5 (17.9–25.0)	73.0 (71.3–75.2)	0.2 (0.0–0.5)
Granules + BMA ($n = 7$)	28.8 (22.4–43.9)	70.2 (41.5–73.8)	0.2 (0.1–0.4)
BAG ($n = 7$)	35.8 (19.4–43.4)	51.1 (48.3–58.56)	0.0 (0.0–1.0)

BAG = bioreactor activated graft material; BMA = bone marrow aspirate.
[a] Data are presented as [median (range)]. No significant differences between groups were observed.

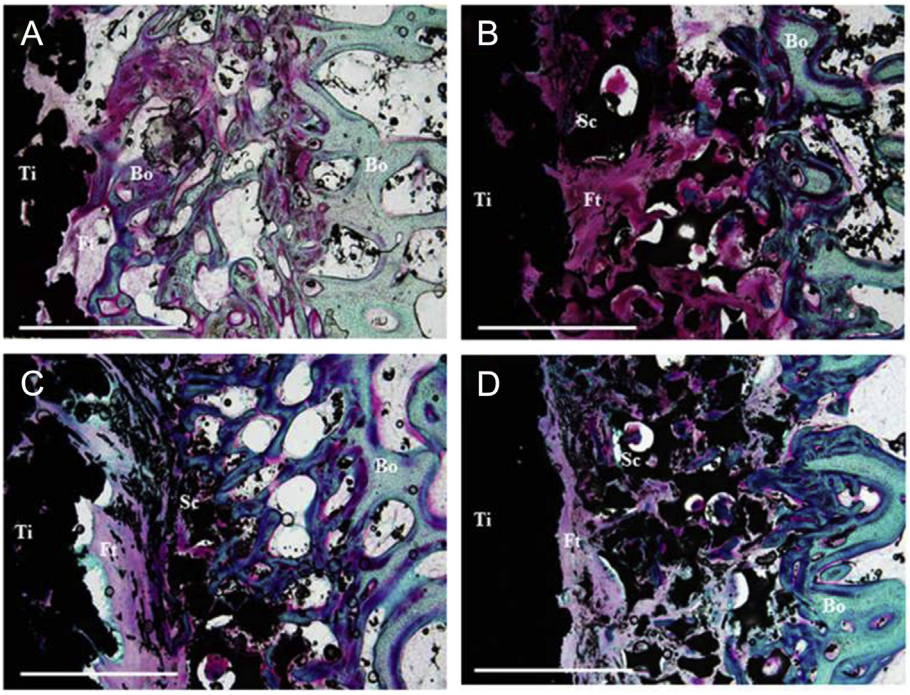

Figure 2 Representative histology from implant pairs in the same sheep. (A) Allograft; (B) granules; (C) granules + bone marrow aspirate; and (D): bioreactor activated graft material. The white scale bar indicates 500 μm. Bo = bone; Ft = fibrous tissue; Sc = scaffold granules; Ti = titanium alloy implant.

Table 5 Mechanical push-out testing: stiffness, strength, and failure energy.

	Stiffness (MPa)[a]	Strength (MPa)[a]	Failure energy (kJ/m^2)[a]
Allograft ($n = 6$)	0.28 (0.17–0.38)	0.06 (0.05–0.09)	16.0 (11.8–22.0)
Granules ($n = 7$)	0.14 (0.11–0.21)	0.04 (0.03–0.09)	17.5 (9.20–24.2)
Granules + BMA ($n = 6$)	0.10 (0.08–0.14)	0.03 (0.02–0.04)	6.74 (5.70–7.71)
BAG ($n = 7$)	0.09 (0.04–0.12)	0.02 (0.01–0.07)	7.71 (7.43–27.6)
p* (Kruskal–Wallis)	$p = 0.096$	$p = 0.383$	$p = 0.334$

BAG = bioreactor activated graft material; BMA = bone marrow aspirate.
* No significant differences between groups were observed.
[a] Data are presented as median (range).

Mechanical testing

The results from the mechanical push-out test (Table 5) showed no significant differences between groups regarding shear stiffness, maximum shear strength, and failure energy.

Discussion

The ideal bone substitute for fixation of larger implants should hold several characteristics including osteoconductivity, osteoinductivity, and osteogenicity. Osteoconductivity ensures the guiding of new bone growth and ultimately assures mechanical stability. Osteoinductivity can be obtained by adding cells with osteogenic potential such as BMSC. The concept of a joint incubation of BMSC and a porous ceramic scaffold for creation of a bone substitute with the above-mentioned properties has been proved [38,39]. However, a large-scale production of viable bone substitutes in a perfusion bioreactor for implantation in critically sized defects has to our knowledge not yet been tried. This study aimed at producing large viable bone grafts activated in a perfusion bioreactor for early implant fixation. This study used a large sheep model with bone properties similar to human bone [40], and allowed us to compare four different groups of materials in each animal; thus, minimising biological variation between animals [8]. The results of this study revealed that bioreactor activated graft material did not convincingly induce early bone formation similar to allograft, although nice early bone formation and implant fixation were observed in all groups.

The fabrication of scaffold granules used in this study was designed to bear porosities and interconnected pore sizes that are highly compatible with bone ingrowth [41]. Hence, new bone formation could be observed within the pores of the scaffold granules as visualised with histology. The coating of scaffold granules with PLA is not assumed to have a negative effect on bone formation, as PLA has been used as a biomaterial for many years. We have recently demonstrated that excellent bone formation in the combining PLA coated scaffold granules with BMSC incubated in a perfusion bioreactor [8].

Living cells with proliferative potential were prerequisite for activation of the scaffold granules. The total numbers of CFU-fs from BMA in five sheep had reached the suggested minimum level for bone formation, while three sheep did not. The bone formation in the concentric gap in these sheep was not significantly different compared with the other animals. Unlike *in vitro* conditions where the culture environment was well-controlled, the *in vivo* environment was far more complicated, e.g., bone formation could be influenced by blood supply, cells, and growth factors released from the host bone etc. Thus, it is likely that CFU-fs may not be the only factor predicting bone formation *in vivo*.

Microarchitectural analysis revealed that bone formations in the allograft and the BAG groups were significantly greater compared with the granule + BMA group. Thus, adding BMA to substitute did not show any additional positive effect on bone formation. Furthermore, the structure of the allograft group was typically plate-like, and the structures of the other three groups were more rod-like or combination of plate and rod. This newly formed bone tissues within the gap (mainly woven bone) might take some time to remodel to become lamellar bone. The TbTh and the connectivity were not different among the four groups.

The microarchitectural parameters of the implanted graft materials largely supported the findings from histomorphometry regarding bone formation. The results for bone formation as evaluated by histomorphometry were separated in two zones, whereas the results from microarchitectural analysis did not discriminate between zones. Implanting allograft still resulted in a higher formation of bone. When comparing the three substitute groups, the granule + BMA group was lowest in bone formation by microarchitectural analysis. By histomorphometry, the bone formation in the granule + BMA group was significantly lower than in the allograft, but not statistically different compared with the other two granule groups. A previous study at our research laboratory has shown that biopolymer coating alters the mechanical and structural properties of a mineral scaffold [21].

For the PDLLA-reinforced scaffold granules, push-out tests showed no significant differences between groups. This finding was supported by the histomorphometric results assessing ingrowth at the tissue–implant interphase. The formation of fibrous tissue in the gap was prominent for all graft materials, whereas bone formation only counted for approximately 20–30%. The bioreactor activated graft material as well as granules with BMA induced more bone and less fibrous tissue formation than seen with the other two graft materials. This difference is, however, not statistically significant.

The coating of scaffold granules with PDLLA is not assumed to have a negative effect on bone formation, as PDLLA have been used as a biomaterial for years. Recent published data from our research laboratory show bone formation combining PDLLA coated scaffold granules with BMSC incubated in a perfusion bioreactor [42]. However, a study has shown delayed osteoinduction and, therefore, less bone formation on composite PDLLA coated scaffolds consisting of HA/β-TCP [43]. The scaffold granules were infiltrated with PDLLA in order to increase the mechanical strength of the material. This was done without compromising the microarchitecture of the scaffold granules [21]; thus, preserving the osteoinductive potential of the scaffold granules. Even though the scaffold materials were not tested against each other, no differences between the properties of the implanted scaffold granules could be concluded; thus, a PDLLA coated scaffold material could be an interesting alternative to allograft for implantation in weight bearing areas.

The remodelling phases of the implanted allograft were examined using histology, and were in full accordance with the results from histomorphometry. Several limitations need to be pointed out.

Firstly, the embedment technique and preparation of the slides for histomorphometry resulted in several artefacts in the tissue. This was especially evident for the groups treated with scaffold granules. The nonresorbed granules were very loosely fitted in the tissue and loosening granules might have resulted in loosening of the adjacent tissues. Therefore, the tissue fractions quantified with μCT scanning are probably more unbiased and closer to the true values. Secondly, like all other preclinical animal studies, the results should be interpreted with caution, and a relatively small sample size might also compromise the significance of the investigation. Nevertheless, the strength of this study was the pair design that compared four scaffold granules within each animal minimising biological variations commonly seen in animal studies, and a novel bioreactor was used to assess the hypothesis that bioreactor might promote bone formation and implant fixation. Bioreactor incubation of scaffold granules with BMSC did not result in significantly more bone formation than granules implanted with no cells. This gives reason to speculate that bioreactor activation is redundant, and that the design and ultimately osteoinductive properties of the scaffold used, is imperative for early bone induction and integration in as proposed by other studies [44,45].

Conclusion

In summary, this study did not support the hypothesis that the BAG could enhance early bone formation in a critically sized defect in sheep. Although bone formation in the gap in the allograft group was significantly greater than in the other three substitute groups, the bone ingrowth into the porous titanium implant was not different, nor the shear mechanical properties. Taken together, BAG did not convincingly induce early implant fixation similar to allograft. This study suggests that neither bioreactor nor by adding BMA credited additional benefit for bone formation in this model.

Conflicts of interest

The authors have no conflicts of interest.

Funding/support

We appreciate the Danish Technological Institute and Fin-Ceramica Faenza for providing scaffold granules. Titanium alloy implants were unconditionally donated by Biomet Inc. This study was mainly supported by the Sixth European Framework Program (Project "AUTOBONE", Grant No. NMP3-CT-2003-505711), and partially supported by the Bevica Fonden.

Acknowledgements

We thank Gitte Reinberg for excellent laboratory work concerning preparation of cells, setting up the bioreactors, preparing histological sections, and also for assistance during and after surgery.

References

[1] Forster Y, Rentsch C, Schneiders W, Bernhardt R, Simon JC, Worch H, et al. Surface modification of implants in long bone. Biomatter 2012;2:149—57.
[2] Stadlinger B, Bierbaum S, Grimmer S, Schulz MC, Kuhlisch E, Scharnweber D, et al. Increased bone formation around coated implants. J Clin Periodontol 2009;36:698—704.
[3] Sittichokechaiwut A, Edwards JH, Scutt AM, Reilly GC. Short bouts of mechanical loading are as effective as dexamethasone at inducing matrix production by human bone marrow mesenchymal stem cell. Eur Cell Mater 2010;20:45—57.
[4] Vetsch JR, Muller R, Hofmann S. The evolution of simulation techniques for dynamic bone tissue engineering in bioreactors. J Tissue Eng Regen Med 2015;9:903—17.
[5] Cancedda R, Giannoni P, Mastrogiacomo M. A tissue engineering approach to bone repair in large animal models and in clinical practice. Biomaterials 2007;28:4240—50.
[6] Goldstein AS, Juarez TM, Helmke CD, Gustin MC, Mikos AG. Effect of convection on osteoblastic cell growth and function in biodegradable polymer foam scaffolds. Biomaterials 2001;22:1279—88.
[7] Allori AC, Sailon AM, Warren SM. Biological basis of bone formation, remodeling, and repair-part II: extracellular matrix. Tissue Eng Part B Rev 2008;14:275—83.
[8] Ding M, Henriksen S, Martinetti R, Overgaard S. 3D perfusion bioreactor activated porous scaffold granules on implant fixation and early bone formation in sheep. Submitted 2015.
[9] Bancroft GN, Sikavitsas VI, Mikos AG. Design of a flow perfusion bioreactor system for bone tissue-engineering applications. Tissue Eng 2003;9:549—54.
[10] Sailon AM, Allori AC, Davidson EH, Reformat DD, Allen RJ, Warren SM. A novel flow-perfusion bioreactor supports 3D dynamic cell culture. J Biomed Biotechnol 2009;2009:873816.
[11] Gomes ME, Sikavitsas VI, Behravesh E, Reis RL, Mikos AG. Effect of flow perfusion on the osteogenic differentiation of bone marrow stromal cells cultured on starch-based three-dimensional scaffolds. J Biomed Mater Res A 2003;67:87—95.
[12] Sikavitsas VI, Bancroft GN, Lemoine JJ, Liebschner MA, Dauner M, Mikos AG. Flow perfusion enhances the calcified matrix deposition of marrow stromal cells in biodegradable

nonwoven fiber mesh scaffolds. Ann Biomed Eng 2005;33:63—70.
[13] Meinel L, Karageorgiou V, Fajardo R, Snyder B, Shinde-Patil V, Zichner L, et al. Bone tissue engineering using human mesenchymal stem cells: effects of scaffold material and medium flow. Ann Biomed Eng 2004;32:112—22.
[14] Lacroix D, Planell JA, Prendergast PJ. Computer-aided design and finite-element modelling of biomaterial scaffolds for bone tissue engineering. Philos Trans A Math Phys Eng Sci 2009;367:1993—2009.
[15] Overgaard S, Lind M, Rahbek O, Bunger C, Soballe K. Improved fixation of porous-coated versus grit-blasted surface texture of hydroxyapatite-coated implants in dogs. Acta Orthop Scand 1997;68:337—43.
[16] Babiker H, Ding M, Sandri M, Tampieri A, Overgaard S. The effects of bone marrow aspirate, bone graft, and collagen composites on fixation of titanium implants. J Biomed Mater Res B Appl Biomater 2012;100:759—66.
[17] Braccini A, Wendt D, Farhadi J, Schaeren S, Heberer M, Martin I. The osteogenicity of implanted engineered bone constructs is related to the density of clonogenic bone marrow stromal cells. J Tissue Eng Regen Med 2007;1:60—5.
[18] Ding M, Henriksen SS, Wendt D, Overgaard S. An automated perfusion bioreactor for the streamlined production of engineered osteogenic grafts. J Biomed Mater Res B Appl Biomater 2015 May 7. http://dx.doi.org/10.1002/jbm.b.33407 [Epub ahead of print].
[19] Martin I, Muraglia A, Campanile G, Cancedda R, Quarto R. Fibroblast growth factor-2 supports *ex vivo* expansion and maintenance of osteogenic precursors from human bone marrow. Endocrinology 1997;138:4456—62.
[20] Ding M, Rojskjaer J, Cheng L, Theilgaard N, Overgaard S. The effects of a novel-reinforced bone substitute and Colloss(R)E on bone defect healing in sheep. J Biomed Mater Res B Appl Biomater 2012;100:1826—35.
[21] Henriksen SS, Ding M, Vinther Juhl M, Theilgaard N, Overgaard S. Mechanical strenght of ceramic scaffolds reinforced with biopolymers is comparable to that of human bone. J Mater Sci Mater Med 2011;22:1111—8.
[22] Ding M, Andreasen CM, Dencker ML, Jensen AE, Theilgaard N, Overgaard S. Efficacy of a small cell-binding peptide coated hydroxyapatite substitute on bone formation and implant fixation in sheep. J Biomed Mater Res A 2015;103:1357—65.
[23] Overgaard S, Soballe K, Jorgen H, Gundersen G. Efficiency of systematic sampling in histomorphometric bone research illustrated by hydroxyapatite-coated implants: optimising the stereological vertical-section design. J Orthop Res 2000;18:313—21.
[24] Ruegsegger P, Koller B, Muller R. A microtomographic system for the nondestructive evaluation of bone architecture. Calcif Tissue Int 1996;58:24—9.
[25] Ding M, Dalstra M, Danielsen CC, Kabel J, Hvid I, Linde F. Age variations in the properties of human tibial trabecular bone. J Bone Joint Surg Br 1997;79:995—1002.
[26] Ding M, Danielsen CC, Hvid I. Age-related three-dimensional microarchitectural adaptations of subchondral bone tissues in guinea pig primary osteoarthrosis. Calcif Tissue Int 2006;78:113—22.
[27] Hildebrand T, Laib A, Muller R, Dequeker J, Ruegsegger P. Direct three-dimensional morphometric analysis of human cancellous bone: microstructural data from spine, femur, iliac crest, and calcaneus. J Bone Miner Res 1999;14:1167—74.
[28] Hildebrand T, Ruegsegger P. Quantification of bone microarchitecture with the Structure Model Index. Comput Methods Biomech Biomed Engin 1997;1:15—23.
[29] Odgaard A, Gundersen HJ. Quantification of connectivity in cancellous bone, with special emphasis on 3-D reconstructions. Bone 1993;14:173—82.
[30] Ding M, Hvid I. Quantification of age-related changes in the structure model type and trabecular thickness of human tibial cancellous bone. Bone 2000;26:291—5.
[31] Baddeley AJ, Gundersen HJ, Cruz-Orive LM. Estimation of surface area from vertical sections. J Microsc 1986;142:259—76.
[32] Babiker H, Ding M, Overgaard S. Demineralised bone matrix and human cancellous bone enhance fixation of porous-coated titanium implants in sheep. J Tissue Eng Regen Med 2015. http://dx.doi.org/10.1002/term.1685 [In press].
[33] Gundersen HJ, Bendtsen TF, Korbo L, Marcussen N, Moller A, Nielsen K, et al. Some new, simple and efficient stereological methods and their use in pathological research and diagnosis. APMIS 1988;96:379—94.
[34] Jensen TB, Rahbek O, Overgaard S, Soballe K. No effect of platelet-rich plasma with frozen or processed bone allograft around noncemented implants. Int Orthop 2005;29:67—72.
[35] Jensen TB, Overgaard S, Lind M, Rahbek O, Bunger C, Soballe K. Osteogenic protein 1 device increases bone formation and bone graft resorption around cementless implants. Acta Orthop Scand 2002;73:31—9.
[36] Jensen PR, Andersen TL, Soe K, Hauge EM, Bollerslev J, Amling M, et al. Premature loss of bone remodeling compartment canopies is associated with deficient bone formation: a study of healthy individuals and patients with cushing's syndrome. J Bone Miner Res 2012;27:770—80.
[37] Braccini A, Wendt D, Farhadi J, Schaeren S, Heberer M, Martin I. The osteogenicity of implanted engineered bone constructs is related to the density of clonogenic bone marrow stromal cells. J Tissue Eng Regen Med 2007;1:60—5.
[38] Braccini A, Wendt D, Jaquiery C, Jakob M, Heberer M, Kenins L, et al. Three-dimensional perfusion culture of human bone marrow cells and generation of osteoinductive grafts. Stem Cells 2005;23:1066—72.
[39] Scaglione S, Braccini A, Wendt D, Jaquiery C, Beltrame F, Quarto R, et al. Engineering of osteoinductive grafts by isolation and expansion of ovine bone marrow stromal cells directly on 3D ceramic scaffolds. Biotechnol Bioeng 2006;93:181—7.
[40] Martini L, Fini M, Giavaresi G, Giardino R. Sheep model in orthopedic research: a literature review. Comp Med 2001;51:292—9.
[41] Hulbert SF, Young FA, Mathews RS, Klawitter JJ, Talbert CD, Stelling FH. Potential of ceramic materials as permanently implantable skeletal prostheses. J Biomed Mater Res 1970;4:433—56.
[42] Sorensen JR, Koroma KE, Ding M, Wendt D, Jespersen S, Juhl MV, et al. Effects of a perfusion bioreactor activated novel bone substitute in spine fusion in sheep. Eur Spine J 2012;21:1740—7.
[43] Habibovic P, Kruyt MC, Juhl MV, Clyens S, Martinetti R, Dolcini L, et al. Comparative *in vivo* study of six hydroxyapatite-based bone graft substitutes. J Orthop Res 2008;26:1363—70.
[44] Habibovic P, Yuan H, van den Doel M, Sees TM, van Blitterswijk CA, de Groot K. Relevance of osteoinductive biomaterials in critical-sized orthotopic defect. J Orthop Res 2006;24:867—76.
[45] Yuan H, Fernandes H, Habibovic P, de Boer J, Barradas AM, de Ruiter A, et al. Osteoinductive ceramics as a synthetic alternative to autologous bone grafting. Proc Natl Acad Sci U S A 2010;107:13614—9.